FEM STRESS ANALYSIS OF HIGH-PRESSURE WIRE REINFORCED HOSES

L. Molnár, K. Váradi, and F. Kovács*

Institute of Machine Design,
Technical University, H-1521, Budapest
Received December 7, 1989.
Presented by Prof. Dr. L. Varga

Abstract

The program system developed for the stress analysis of fibre reinforced hoses reckoning with material and geometrical nonlinearities suits analysis of hoses exposed to internal pressure, axial force, bending moment, or to any combination of them. Computed and measured results for a hose specimen of simple structure have been compared, and strain and stress states of a hose of complex structure exposed to internal pressure analyzed.

Studies on wire reinforced hoses have been made at the Institute of Machine Design, TUB, on commission by the Taurus Rubber Works.

Introduction

Wire reinforced hoses are mostly applied for conveying water, oil, etc. at a very high pressure (10 to 50 MPa). In designing these hoses, the arrangement of reinforced layers and coiling angle of strands have to be chosen so that when exposed to an internal pressure, the hose undergoes as little axial deformation and torsion as possible, while strands are about uniformly loaded.

Another requirement for the hose is to be flexible enough for coiling. Meeting the outlined design requirements is conditioned by a thorough analysis of the strength behaviour of hoses relying on mechanical models of composite materials.

Composite materials are systems of different materials with novel material characteristics — anisotropic as a rule ([1], [2]).

FEM is a current method for the design of structures built up of composite materials. Theoretically it suits strength analysis of structures with an arbitrary number of anisotropic layers, in domains of both material nonlinearity and high

deformability. At the same time, only the topmost FEM systems suit a sophisticated analysis. "Medium" or minicomputer systems — such as that to be presented — suit analysis only under approximate assumptions.

1. Mechanical modelling of a hose as a composite structure, and the FEM algorithm

Material characteristics and isotropy for wire reinforced hoses (Fig. 1) show fundamental differences between layers.

The stiffness behaviour of a hose is determined, first of all, by layers containing the reinforcement. In these layers the directional angle of the strand is an essential
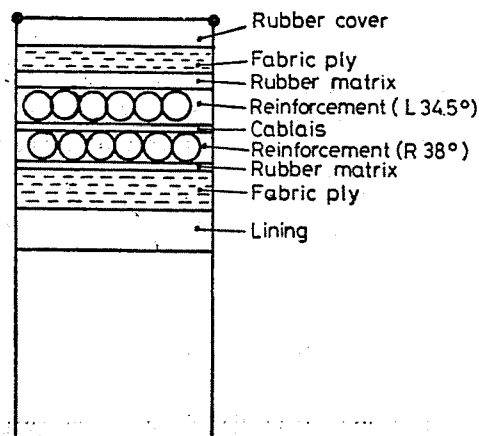
Fig. 1

design parameter, its variation decisively influencing the stiffness, stress and strain condition of the hose. An approximation accepted in the mechanical modelling of the reinforced layer is to replace the two components of the layer by a single homogeneous anisotropic material, with material characteristics composed from those of the actual two materials it replaces.

1.1. Anisotropic material matrix and material characteristics

In knowledge of isotropic and anisotropic material characteristics of any layer of a composite material, material matrices of each layer can be established, then equilibrium relationships of the composite structure, or the proper numerical solution methods, may help to determine the displacement, strain and stress state wanted.

Let us consider the linear elastic material law between strain and stress tensors for an orthotropic case, in principal directions 1, 2 and 3 of the material:

$$
\begin{bmatrix}
\varepsilon_{11} \\
\varepsilon_{22} \\
\varepsilon_{33} \\
\gamma_{12} \\
\gamma_{23} \\
\gamma_{31}
\end{bmatrix}
=
\begin{bmatrix}
\dfrac{1}{E_1} & -\dfrac{\nu_{21}}{E_2} & -\dfrac{\nu_{31}}{E_3} & \emptyset & \emptyset & \emptyset \\
-\dfrac{\nu_{12}}{E_1} & \dfrac{1}{E_2} & -\dfrac{\nu_{32}}{E_3} & \emptyset & \emptyset & \emptyset \\
-\dfrac{\nu_{13}}{E_1} & -\dfrac{\nu_{23}}{E_2} & \dfrac{1}{E_3} & \emptyset & \emptyset & \emptyset \\
\emptyset & \emptyset & \emptyset & \dfrac{1}{G_{12}} & \emptyset & \emptyset \\
\emptyset & \emptyset & \emptyset & \emptyset & \dfrac{1}{G_{23}} & \emptyset \\
\emptyset & \emptyset & \emptyset & \emptyset & \emptyset & \dfrac{1}{G_{31}}
\end{bmatrix}
\begin{bmatrix}
\sigma_{11} \\
\sigma_{22} \\
\sigma_{33} \\
\tau_{12} \\
\tau_{23} \\
\tau_{31}
\end{bmatrix}
$$

(The relationship contains moduli of elasticity, Poisson's ratios, and shear moduli of elasticity interpreted in principal material directions.)

The constants of the material laws vary from layer to layer, e.g., for the reinforced layer they can be produced from material characteristics of the rubber matrix and the strand. The special literature contains many formulae for the actual determination concerned (e.g. [1], [3], etc.). They have in common that the volume ratios of the component materials are taken into account.

The formulae mentioned refer to only small deformations. In the analysis of the stiffness behaviour of the hose, however, a nonlinear variation of anisotropic material characteristics has to be assumed. Its determination vs. deformation may rely on the Mooney—Rivlin theory, taking the strain energy of the rubber into consideration.

1.2. Ultimate characteristics

The final aim of the design of wire reinforced hoses is to achieve a hose structure either the most reliable to bear a definite load, or, of the highest load capacity.

Table 1

Nr.	Ultimate characteristics	Remark
I	$(\sigma_{11}^+)^*$, $(\sigma_{11}^-)^*$	Strand failure
II	$(\tau_{12})^*$	Strand slip
III	$(\varepsilon_{22}^+)^*$, $(\varepsilon_{22}^-)^*$, $(\gamma_{12})^*$	Rubber matrix damage
IV	$\tau_{\text{interface}}^*$	Interface separation
V	Loss of stability	
VI	Fatigue	Repeated stresses

The ultimate characteristics of wire reinforced hoses are summarized in Table 1, where the values marked by an * are ultimate stresses or strain characteristics typical of the given mode of failure. For instance, ultimate stress $(\sigma_{11}^+)^*$ is typical of tension in principal material direction 1.

1.3. FEM Algorithm

To examine the structural behaviour of anisotropic structures with nonlinear material and geometric characteristics, an approximate algorithm has been developed, using small load steps, determining for the load steps the increments of displacements, strains, and stresses, to be summed up. Strain and stress states are determined in the coordinate system of their principal material direction. In every load step, the geometry of the structure, coiling angle of the strand in conformity with the deformation, just as all material characteristics, are changing.

2. Analysis and testing of the hose specimen

To check the developed algorithm, measurements and analyses have been made on a hose consisting of the following four layers:

— Inner rubber layer $(R_b=50.1$ mm)
— Reinforcement 37° $(R_b=52$ mm)
— Reinforcement −36° $(R_b=54.35$ mm)
— Rubber cover $(R_b=56.7$ mm)
        $(R_k=58.8$ mm).

Material characteristics for each layer have been determined from measurements by computation or by estimation.
For the rubber layer: $E=4.5$ MPa, $\nu=0.49$.
For the reinforcement:

$$E_{11}=140\,000\text{MPa}, \qquad E_{22}=22\text{ MPa}, \qquad E_{33}=13\text{ MPa},$$
$$\nu_{12}=0.4 \qquad\qquad \nu_{13}=0.4 \qquad\qquad \nu_{23}=0.46$$
$$G_{12}=6\text{ MPa}, \qquad\qquad G_{13}=6\text{ MPa}, \qquad\qquad G_{23}=6\text{ MPa}.$$

As the first load case, the effect of the bending moment has been examined. The test arrangement is shown in Fig. 2. The tested hose length has been fixed below, and the pure moment load has been applied as shown in Fig. 2. Measurement results are presented in Figs 3a, b, c. Measured maxima and minima have been plotted in thin lines, while the computation results in thick lines. Figures 3a and b show hose end displacements in directions y and z, respectively. Measurements have been made on hose elongations (or compressions) in the tensile or compressed side. In confor-
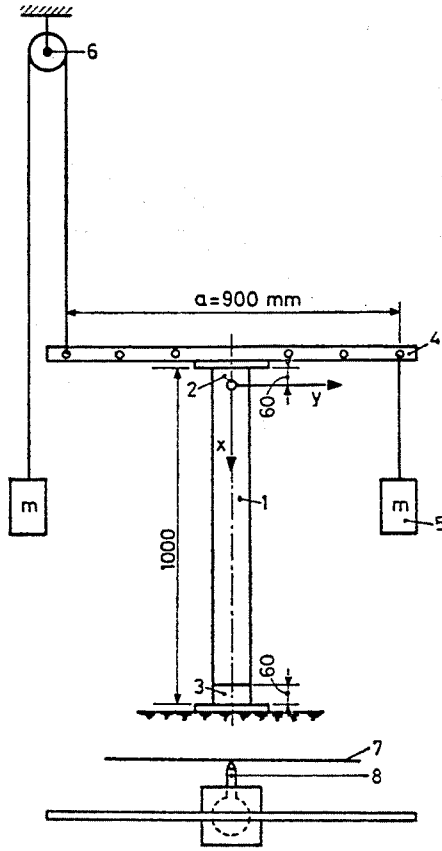
Fig. 2
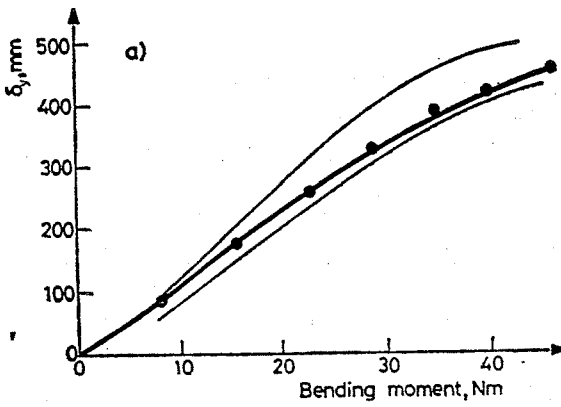
Fig. 3. a
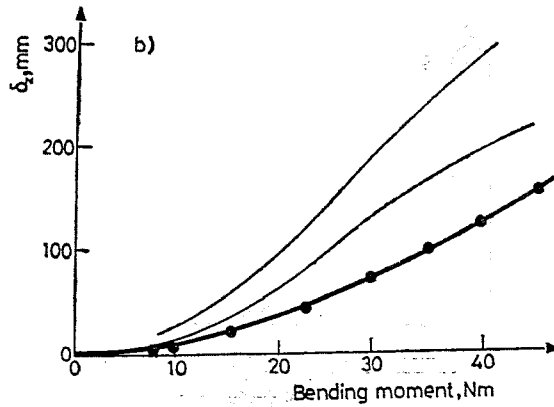
Fig. 3. b
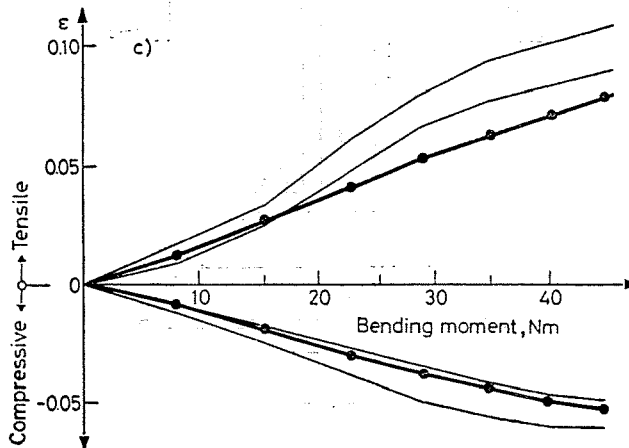
Fig. 3. c

mity with Fig. 3c, deformation is "softer" in the tensile than in the compressed side. All three of the deformation characteristics have also been determined by computations (in thick lines). The agreement is likely to improve for denser FEM meshes and for smaller load steps.

Strains and stresses in each hose layer have been interpreted in the coordinate system of principal material directions. Principal material direction 1 is the strand direction in the reinforcement. Figure 4 shows stresses σ_{11} in the outer and inner reinforcements. According to the figure, practically no stress arises in the strands either on the tensile or on the compressed side, but only about the neutral axes where strands exhibit increasing compressive stresses in conformity with the elliptic hose cross section. The axonometric view of the bent hose is shown in Fig. 5.
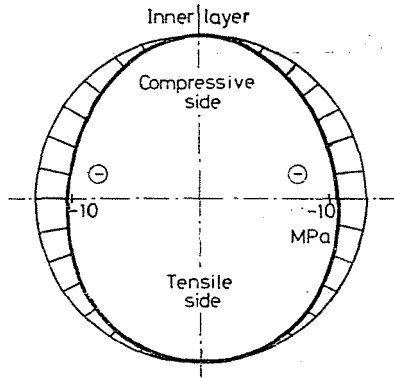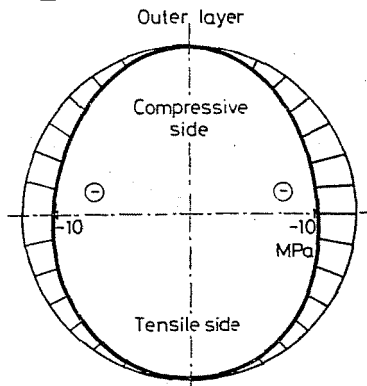
Fig. 4
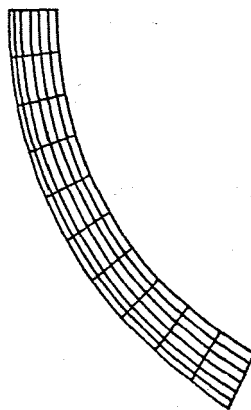
Fig. 5
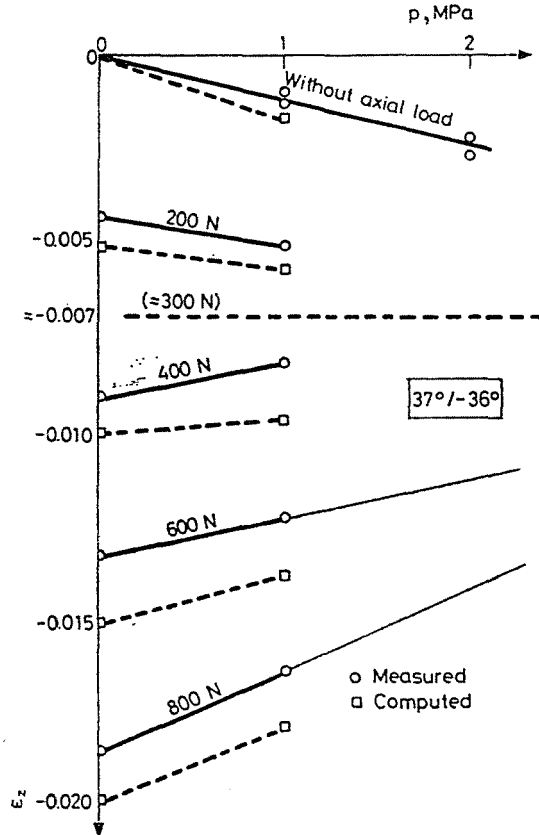
Fig. 6

Axial deformation of a hose exposed to *internal pressure* and *axial force* is seen in Fig. 6. Axial compression of the hose under axial load (200 N, 400 N, 600 N, and 800 N) as well as under combined axial load and internal pressure has been examined. Figure 6 shows a fair agreement between computed and measured values. According to this figure, an axial force of about 300 N results in an equilibrium condition where the hose exposed to internal pressure is exempt from axial displacement.

3. Stress/Strain Condition of the hose exposed to internal pressure

The hose layered as seen in Fig. 1 has been analyzed by means of four-layer and eight-layer FEM models. In the four-layer model, layers 1, 2, 7, 8 and 9 have been considered as rubber matrix-type layers, while the eight-layer model has also reckoned with plies. Plies had to be considered as two finite element layers each, since compound fibre orientations $+45°/-45°$ could only be reckoned with separately ($+45°$ or $-45°$).

Layer radii of the eight-layer model:
Inner radius of
  — core: 31.75 mm
  — ply (45°): 36.25 mm
  — ply (−45°): 37.79 mm
  — reinforcement (34.5°): 39.33 mm
  — reinforcement (38°): 39.33 mm
  — ply (45°): 48.63 mm
  — ply (−45°): 50.34 mm
  — rubber cover: 52.05 mm
outer radius of rubber cover: 55.55 mm.
Length of the hose modelled: 500 mm.

The program developed for generating the field of data has produced the due boundary conditions, and yielded the necessary internal pressure and axial force values for the given elements.

The incremental computation set involved first 0.2 MPa load steps, then continuously increasing load steps. Axial load:

$$F_{ax} = A_0 p = 31.75^2 \cdot \pi \cdot 0.2 = 633 \, \text{N}$$

distributed among nodes of the reinforcement.

Material characteristics for each layer:

Rubber matrix:
$$E_g = 7.8 \, \text{MPa}, \qquad v = 0.49$$

Ply:
  — rubber matrix: $E_g = 7.8$ MPa,
  — fibre: $E = 4000$ MPa.
  — cover: 0.5 and 0.5
  — $v_{12} = 0.49$; $v_{13} = 0.49$; $v_{23} = 0.49$

Reinforcement:
  — rubber matrix: $E_g = 4.5$ MPa,
  — strand: $E = 38\,600$ MPa,
  — cover: 0.92 and 0.92,
  — $v_{12} = 0.4$; $v_{13} = 0.4$; $v_{23} = 0.46$.

3.1. Consideration of the effect of internal pressure acting in reinforcement layers between strands

Tests made about strand winding angles belonging to the balance condition of the hose showed that axial elongations computed with the FEM model are less (greater in absolute sense) than shown by measurements. In other words, near the

equilibrium condition the model has to be acted upon by a higher axial force than that determined from the pressure and the inner hose diameter. According to measurements, the necessary correction of the axial force is 15 to 20%.

This deviation is likely to be attributed to the difference between real and simulated features of the reinforced layer.
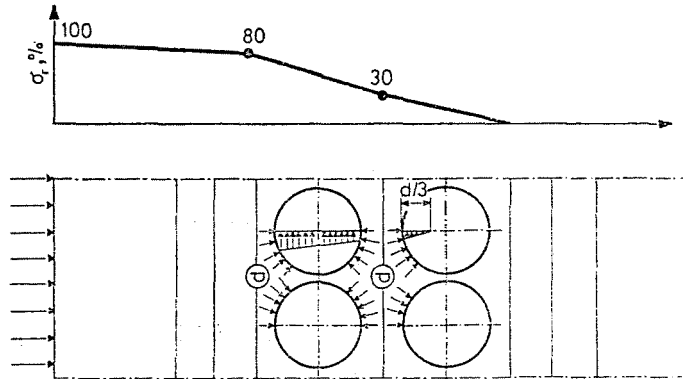
Fig. 7

Let us consider reinforcements and strands in Fig. 7. The FEM model of these layers is a homogeneous and isotropic material structure (rather than strands and rubber matrix) omitting peculiarities. Accordingly, the replacing material structure suits to trace the internal pressure on the element side, and the axial load on the lateral surface, but the element itself is homogeneous. In reality, strands are embedded in rubber matrix developing compression upon an internal pressure. Due to the annular pressure in the bedding rubber acting on the strand wires, these latter undergo elongation, to be reckoned with by an accessory force in the homogeneous model. The outlined effect may be considered as an accessory force.

The value of the accessory force system is estimated from the radial stress σ_R. The nature of σ_R appears from Fig. 7, while its exact variation in each layer of the eight-layer hose is shown in Fig. 8. According to Fig. 7, in inner layers of the hose the spherical stress state is fairly well approximated, while in the reinforcements the stress σ_R abruptly decreases. The shaded area in Fig. 8 shows the estimated distribution of the accessory force system. This stress is taken as 100% in the inner reinforcement, to become zero in the second reinforcement at depth $d/3$. The resultant of the force system corresponding to linear variation is the same as if the accessory force system acted on the reinforcement over a length of $2/3\ d$ in a single reinforcement layer. Thus,

$$F_{ax}^* = (R^2 - r^2)\pi p = (45.2^2 - 42.8^2)\pi \cdot 0.2 = 133\ \text{N}.$$

In the following, results for both F_{ax} and $(F_{ax} + F_{ax}^x)$ will be presented.
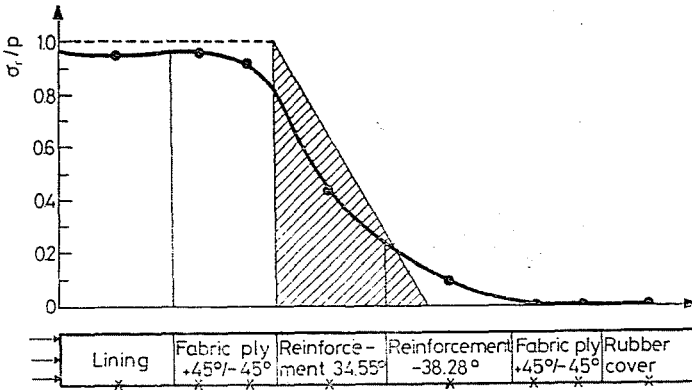
Fig. 8

Obviously, F_{ax}^x as a resultant force cannot be experienced in a real hose structure, since it makes up an equilibrium force system about every strand. At the same time, this is the only way for this FEM model to reckon with the effects outlined above.

3.2. Deformed condition of a 2.5" hose

Axial and radial displacements, as well as angular rotation of the tested hose are shown in Figs 9, 10 and 11.
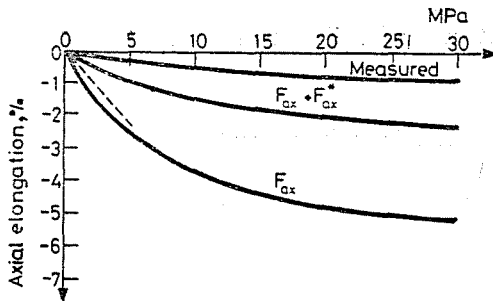
Fig. 9

Graphs F_{ax} show effects of the (nominal) axial force and the internal pressure as interpreted in the previous item. Curves $F_{ax} + F_{ax}^x$ illustrate the effect of force correction. Effects of force F_{ax} and of internal pressure for an eight-layer hose model are plotted in dashed lines. These computations have only been made up to $p = 5$ MPa. The results do not differ significantly from those for four-layer models, at a significant increase of running time. Therefore four-layer models are preferred.
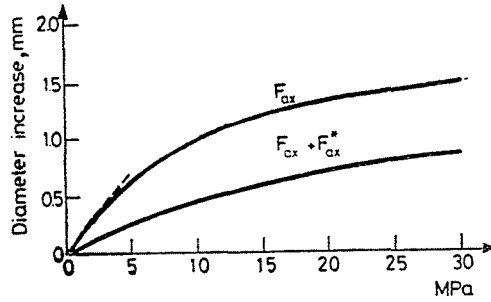
Fig. 10
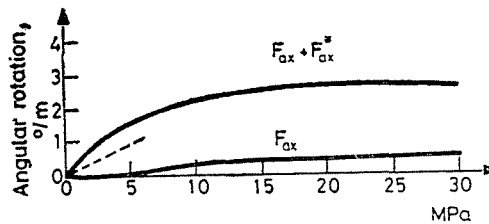
Fig. 11

For F_{ax} and for F_{ax}^x the axial shrinkages of about 5% and 2%, resp., are seen·in Fig. 9. Diameters increase in similar proportions in Fig. 10. Maximum angular rotations are 3 to 4%, while for F_{ax} they are below 1%.

3.3. Stress/strain state of the 2.5" hose

Deformations and stresses in outer and inner reinforcement layers interpreted in principal material directions are shown in Figs 12, 13 and 14. The specific strain and normal stress vary linearly in principal material direction 1. Stresses in outer and inner reinforcement strands differ by about 20%.

According to Fig. 13, stresses and strains in each layer, normal to the strand, are of non-linear character, σ_{22} is much less than σ_{33}.

In Figure 14, on the one hand, σ_{33} in the inner layer of reinforcement, a radial stress, and on the other hand, ε_{33} in the same, are noteworthy. In conformity with fed=0.92, ε_{33} is markedly nonlinear, it tends asymptotically to the value -0.08.

It can be concluded that inc omputations reckoning with F_{ax}^x, the axial displacement of the hose is significantly altered, and the results obtained agree better with test results for axial hose displacements.
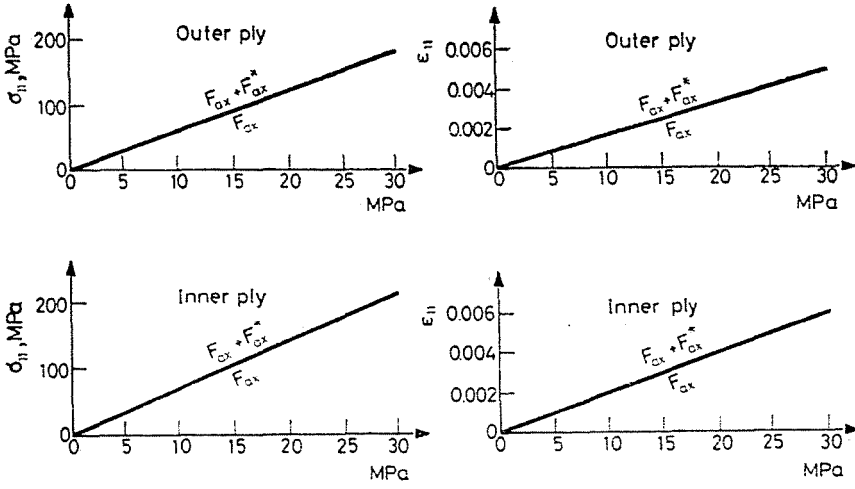
Fig. 12
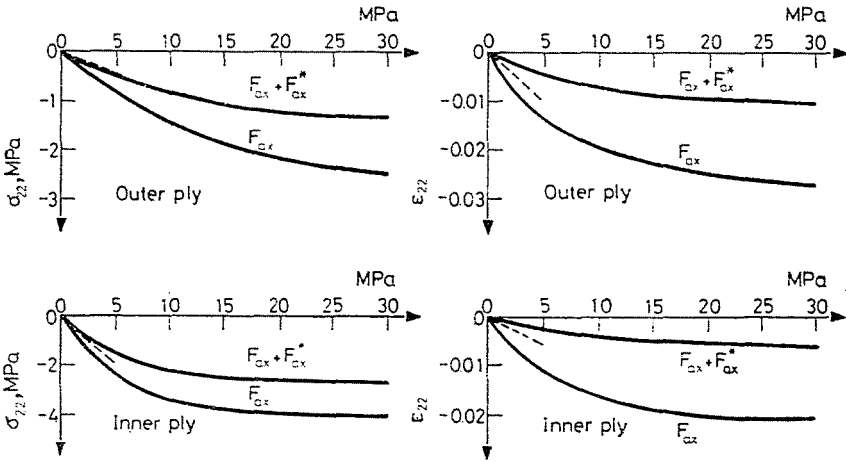
Fig. 13

The value for F_{ax}^x has been determined from the assumption that in Fig. 7 the stress σ_R is zeroed in the second reinforcement layer at a depth of $d/3$. Computations (including those for the hose specimen) support the assumption that the stress σ_R becomes zero at depth d in the second reinforcement layer. This assumption is in close agreement with the 9.5% increment for the hose specimen just as it follows from Fig. 9 and the test results.
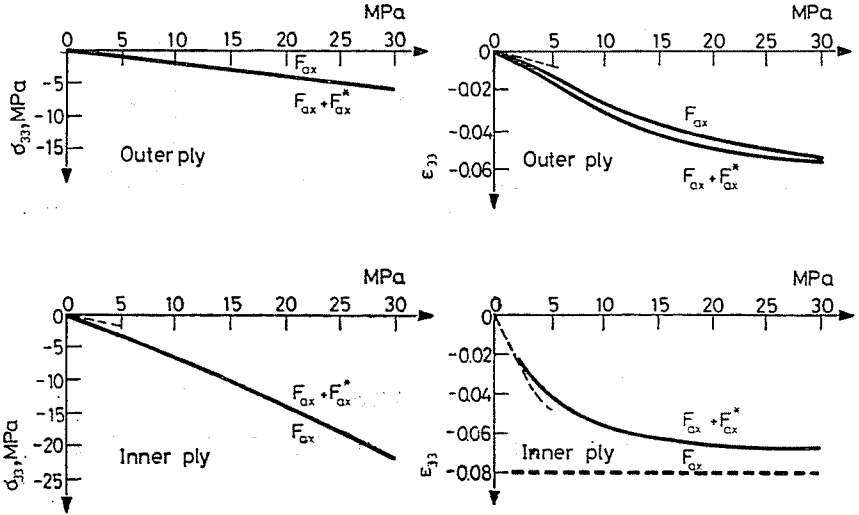
Fig. 14

References

1. VISON, J. R.—SIERAKOWSKI, R. L.: The Behavior of Structures Composed of Composite Materials, Martinus Nijhoff Publishers, 1986.
2. ROUSE, N. E.: "Optimizing Composite Design", Machine Design, February, 25, 1988. pp. 62—65.
3. TABADDOR, F.: "Mechanical Properties of Cord-Rubber Composites" Composite Structures, *3* (1985), pp. 33—53.

László MOLNÁR,
Károly VÁRADI,   } H-1521, Budapest
Ferenc KOVÁCS,